Title
Lead Selenide Nanowires Prepared by Lithographically Patterned Nanowire Electrodeposition

Journal
The Journal of Physical Chemistry Letters, 1(7)

ISSN
1948-7185 1948-7185

Authors
Hujdic, Justin E
Taggart, David K
Kung, Sheng-Chin
et al.

Publication Date
2010-04-01

DOI
10.1021/jz100173a

Peer reviewed

THE JOURNAL OF PHYSICAL CHEMISTRY Letters

pubs.acs.org/JPCL

Lead Selenide Nanowires Prepared by Lithographically Patterned Nanowire Electrodeposition

Justin E. Hujdic,[†] David K. Taggart,[‡] Sheng-Chin Kung,[‡] and Erik J. Menke*[,†]

[†]School of Natural Sciences, University of California, Merced, California 95343 and, and [‡]Department of Chemistry and Institute for Surface and Interface Science, University of California, Irvine, California 92697-2025

ABSTRACT We describe the electrochemical deposition of lead selenide (PbSe) nanowire arrays by the lithographically patterned nanowire electrodeposition (LPNE) method. The nanowires were electrodeposited using a constant potential method from an aqueous solution containing Pb^{2+} and $HSeO_3^-$ at room temperature onto an electrode that had been photopatterned in unfiltered laboratory air. The resulting polycrystalline nanowires were stoichiometric, face-centered cubic PbSe and had a rectangular cross section with lengths > 1 mm, widths between 80 and 600 nm, and heights between 40 and 80 nm. The synthesized nanowires were characterized by scanning electron microscopy (SEM), energy dispersive X-ray fluorescence (EDX), transmission electron microscopy (TEM), selected area electron diffraction (SAED), and powder X-ray diffraction (XRD). The electrical resistivity of the nanowires is comparable to that of other PbSe nanowires.

SECTION Nanoparticles and Nanostructures

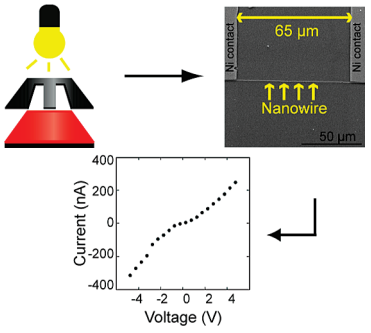

Lead selenide is a 0.27 eV direct band gap material used in devices including infrared detectors,[1−6] thermal-imaging systems,[3−5,7−10] and mid-IR lasers.[11−18] Its small band gap and relatively large exciton Bohr radius of 46 nm also make it a useful model system for studying quantum confinement effects in nanoribbons, nanowires, and nanoparticles. As a practical result of these quantum effects, lead selenide nanoparticles have been proposed as a possible material for future-generation, high-efficiency solar cells,[19−25] although it is still unclear how efficient these effects are at improving solar cells.[26−31]

Due to these potential uses for PbSe nanowires, a number of research groups have prepared PbSe nanowires using a variety of synthetic methods, including (1) vapor−liquid−solid synthesis,[32−34] (2) electrochemical reduction of Pb^{2+} and $HSeO_3^-$,[35−37] (3) chemical reduction of Pb^{2+} in the presence of Se,[38] and (4) chemical vapor transport synthesis.[39] All of these methods have two common drawbacks. The first drawback is that the nanowire length produced by these methods is limited to less than 100 μm in the best cases, with the majority of these methods producing nanowires with lengths less than 1 μm. The second drawback is that these methods generally produce nanowires that are randomly oriented and dispersed on a surface. The net result of these two drawbacks is that any integration or electrical characterization of the nanowires requires nontrivial postsynthesis processing, such as e-beam lithography.

To address these issues, we have prepared lead selenide nanowires via lithographically patterned nanowire electrodeposition (LPNE). LPNE is a multistep nanowire deposition process, developed by the Penner group, that uses photolithography to create a template for nanowire deposition and has been used to prepare gold, platinum, palladium, bismuth, and lead telluride nanowires.[40−42] Briefly, the LPNE method, shown in Scheme 1, consists of seven-steps, (1) Evaporate nickel onto a piece of float glass, (2) coat the nickel film with photoresist, (3) pattern the photoresist, (4) chemically etch away the exposed nickel, undercutting the photoresist to create the deposition template, (5) electrodeposit desired material into the template, (6) remove excess photoresist, and (7) chemically etch away the excess nickel, leaving a free-standing nanowire.

Scheme 1. Seven-Step LPNE Process

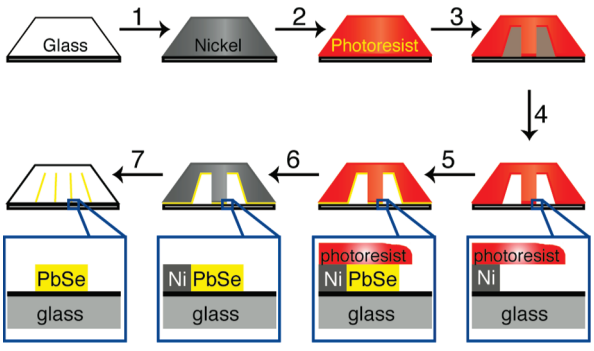

Of these seven steps, the electrodeposition step (step 5) is the most important as it dictates the nanowire material. We synthesized lead selenide nanowires by a constant potential

Received Date: February 7, 2010
Accepted Date: March 2, 2010
Published on Web Date: March 08, 2010

DOI: 10.1021/jz100173a | *J. Phys. Chem. Lett.* **2010**, *1*, 1055–1059

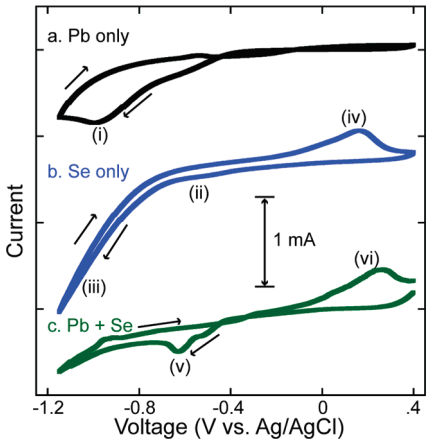

Figure 1. Cyclic voltammograms (20 mV s^{-1}) for solutions containing (a) lead ($[Pb^{2+}]$ = 10 mM) with 0.1 M EDTA at pH = 4 in aqueous solution, (b) selenium ($[HSeO_3^-]$ = 1 mM) with 0.1 M EDTA at pH = 4 in aqueous solution, and (c) lead and selenium ($[Pb^{2+}]$ = 10 mM; $[HSeO_3^-]$ = 1 mM) with 0.1 M EDTA at pH = 4 in aqueous solution. The voltammetric waves are assigned to the following reactions: wave (i), $Pb^{2+} + 2\,e^- \rightarrow Pb^0$; wave (ii), $HSeO_3^- + 5\,H^+ + 4\,e^- \rightarrow Se^0 + 3\,H_2O$; wave (iii), $2\,H_3O^+ + 2\,e^- \rightarrow H_2 + 2\,H_2O$; wave (iv), $Se^0 + 3\,H_2O \rightarrow HSeO_3^- + 5\,H^+ + 4\,e^-$; wave (v), $Pb^{2+} + HSeO_3^- + 5\,H^+ + 6\,e^- \rightarrow PbSe + 3\,H_2O$; wave (vi), $PbSe + 3\,H_2O \rightarrow Pb^{2+} + HSeO_3^- + 5\,H^+ + 6\,e$.

method similar to the method used by Saloniemi et al. to electrodeposit thin PbSe films.[43,44] In our method, PbSe electrodeposition was achieved from an aqueous deposition solution containing 0.1 M Na_2EDTA, 10 mM $Pb(NO_3)_2$, and 1 mM SeO_2, with the final solution pH adjusted to 4 by the dropwise addition of conc. HNO_3. The EDTA and large excess of $Pb(NO_3)_2$, relative to the SeO_2 concentration, are needed to shift the deposition potentials so that the start of the lead reduction (wave (i) in Figure 1a) occurs at approximately the same potential as that of selenium reduction (wave (ii) in Figure 1b). This ensures that lead and selenium are codeposited (wave (v) in Figure 1c) at a potential of approximately −0.6 V versus Ag/AgCl without excess lead or selenium present, as is evidenced by the lack of a second stripping wave in Figure 1c. After the final LPNE step, all that is present on the glass surface is a parallel array of PbSe nanowires, shown in Figure 2a.

The pitch of the nanowire arrays, such as the one shown in Figure 2a, is controlled by the photomask and is ultimately limited by the diffraction limit of the light used for the photolithography. However, both the height and width of the nanowires are independent of the photolithography, as well as each other. The height of the individual nanowires is equal to the thickness of the nickel film that is deposited in step 1 of the LPNE method over a wide range of nickel film thicknesses.[40] However, the nanowire width is dependent on the electrodeposition time, with a rate that depends on the electrodeposited material. In addition, PbSe nanowires have protrusions on the side opposite the nickel electrode, as can be seen in Figure 2b, which grow larger over time, resulting in a larger variation in wire width at longer deposition times. Figure 2c demonstrates that even with this increasing roughness, the width of the resulting nanowires is dependent on the deposition

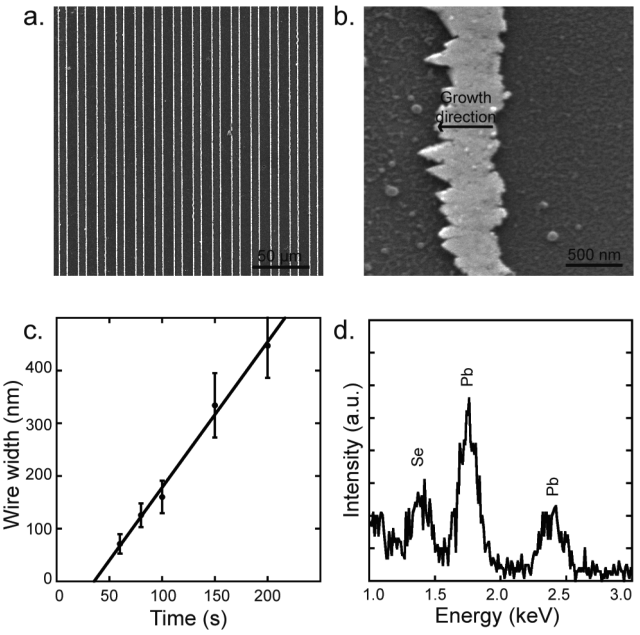

Figure 2. (a) Low-magnification SEM image showing an array of parallel PbSe nanowires with 5 μm separation (scale bar = 50 μm). (b) High-magnification SEM image of a single nanowire after 150 s of deposition (scale bar = 500 nm). (c) Calibration curve of the nanowire width as a function of electrodeposition time. (d) EDX spectra of a single nanowire showing the presence of lead and selenium. The Pb/Se atomic ratio measured by EDX is 50:50.

time with a high degree of control over the resulting nanowire width. The EDX analysis shown in Figure 3d offers evidence of stoichometric PbSe nanowires, as only lead and selenium are present, and they are in an atomic ratio of approximately 1:1.

A single PbSe nanowire, approximately 40 nm in height and 200 nm in width, is shown in the transmission microscope image in Figure 3a. This image displays the nanocrystalline nature of these nanowires, with grain sizes between 20 and 100 nm. Note that the grains closer to the nickel edge (left side of the nanowire) are smaller, as has also been seen in Pd nanowires grown by the LPNE method.[45] Selected area electron diffraction was also performed on this nanowire, with the resulting diffraction pattern shown in Figure 3b. All of the peaks in the diffraction pattern can be indexed to a reference cubic PbSe diffraction pattern, (JCPDS 06-0354, shown in the inset to Figure 3b), demonstrating that the nanowire is made of cubic PbSe. To further ensure that the electrodeposited material was PbSe, an array of 500 nm wide nanowires was prepared, and X-ray diffraction on the resulting array was collected. The resulting diffraction pattern is compared to the standard cubic PbSe diffraction pattern in Figure 3c, again showing that only cubic PbSe is electrodeposited. In addition, Scherrer analysis on the peak widths predicts grain diameters of 53 nm, similar to what was observed by TEM.

Rather than etching the remaining nickel after the electrodeposition step to leave isolated nanowires, an additional photolithography step can be added to selectively etch away only some of the nickel, resulting in a nanowire with nickel contacts, as shown in Figure 4a. This provides a way to perform *IV* measurements on a single PbSe nanowire with

DOI: 10.1021/jz100173a | *J. Phys. Chem. Lett.* **2010**, *1*, 1055–1059

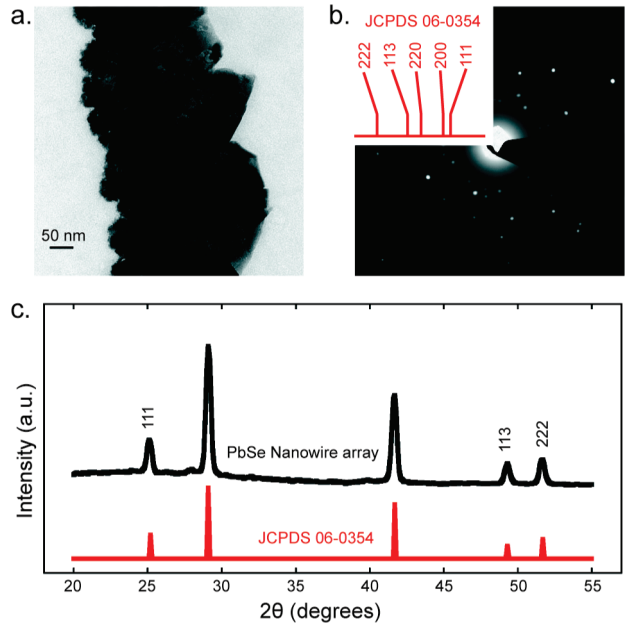

Figure 3. (a) TEM image of a single nanowire showing grain sizes in the 20−100 nm range (scale bar = 50 nm). (b) Selected area electron diffraction of the nanowire with the inner five rings indexed to cubic PbSe (JCPDS 06-0354). (c) X-ray diffraction patterns from an array of 500 nm wide PbSe nanowires and a reference XRD stick pattern for cubic PbSe (JCPDS 06-0354).

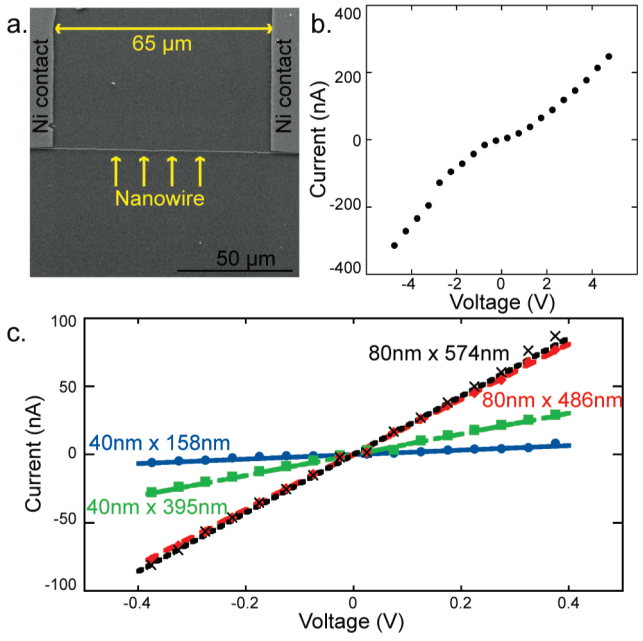

Figure 4. (a) SEM image of a single PbSe nanowire with two nickel contacts. (b) Large bias $I-V$ curve of a single 40 nm (h) × 158 nm (w) × 64 μm (l) PbSe nanowire showing diode-like behavior. (c) Small bias $I-V$ curves of a single PbSe nanowire with dimensions of 40 nm (h) × 158 nm (w) × 64 μm (l) (blue circles), 40 nm (h) × 395 nm (w) × 68.5 μm (l) (green squares), 80 nm (h) × 486 nm (w) × 138 μm (l) (red diamonds), and 80 nm (h) × 574 nm (w) × 98.5 μm (l) (black crosses). The resistivity values for these nanowires are presented in Table 1.

Table 1. Comparison of Electrical Resistivity for PbSe Nanowires with Different Aspect Ratios

sample	height (nm)	width (nm)	length (μm)	resistivity (10^{-3} Ω m)
1	40	158	64	6.0
2	40	395	68.5	3.0
3	80	486	138	1.4
4	80	574	98.5	2.2
ref 39				1.5
ref 46				1.5

heights ranging from 40 to 80 nm, widths ranging from 100 to 600 nm, and lengths from 65 to 150 μm. The *IV* curve on a single nanowire over a large voltage range, shown in Figure 4b, shows diode-like behavior, suggesting that the nickel−PbSe contact is not ohmic. However, over a small bias range, the *IV* curve is linear, as can be seen for four separate nanowires with different aspect ratios in Figure 4c. The resistivities calculated from these *IV* curves are shown in Table 1 and are similar to, although larger than, both the resistivity of a single-crystal PbSe nanowire prepared via VLS by Fardy et al.[39] and a nanowire-like assembly of PbSe nanoparticles prepared via chemical reaction by Sashchiuk et al.[46] The differences between resistivity values are likely due to a combination of grain boundary scattering and oxidation in the LPNE-prepared nanowires as these nanowires are highly nanocrystalline and wires were exposed to ambient air for at least 5 days before the *IV* curves were collected.

In summary, nanocrystalline PbSe nanowires have been prepared by LPNE with independent control over the length, width, and height of the nanowires. These nanowires are stoichometric and single-phase, with electrical resistivities comparable to those of PbSe nanowires prepared via alternative methods. This opens the door to new opportunities for studying both the optical and electronic properties of PbSe nanowires and their potential application in a variety of systems.

EXPERIMENTAL DETAILS

Microscope slides where cut into 1 in. × 1 in. squares and soaked in a Nochromix solution for 24 h. These slides were then rinsed with NANOPure water (resistivity = 18.0 MΩ cm), dried with compressed air, and then placed in a Denton BTT-IV evaporator. Nickel was thermally evaporated at a rate of 0.1 nm sec^{-1} while the nickel thickness was monitored with a SQM-160 film thickness monitor (INFICON). After the nickel had reached the desired thickness, the nickel-coated slides were removed from the evaporator coated with S1808 photoresist (ROHM & HAAS). The resist was photopatterned using an OAI model 30 UV light source, developed in MF-24A (ROHM & HAAS), rinsed in NANOPure water, and dried with compressed air. The photopatterned slides were then placed in a 1 M HNO_3 solution for 5 min to etch the exposed nickel, resulting in a nickel template electrode for the lead selenide electrodeposition.

The electrodeposition of lead selenide nanowires was carried out in a deposition solution containing 0.1 M Na_2EDTA

DOI: 10.1021/jz100173a | J. Phys. Chem. Lett. 2010, 1, 1055–1059

(Sigma Aldrich, Purity 99%), 0.01 M $Pb(NO_3)_2$ (Sigma Aldrich, Purity 99.999%), and 0.001 M SeO_2 (Sigma Aldrich, Purity 99.999%) in NANOPure water at a potential of −0.6 V versus a Ag/AgCl reference electrode. The deposition was carried out on a computer-controlled Gamry Instruments G300 Series potentiostat/galvanostat at room temperature.

The nanowire stoichiometric ratio has been characterized on a Genesis energy-dispersive X-ray (EDAX) spectrometer. The crystallographic data were collected using a Rigaku Ultima III (Rigaku, Tokyo, Japan) high-resolution X-ray diffractometer (XRD) with Cu K irradiation. The X-ray generator was operated at 40 kV and 44 mA. The JADE 7.0 (Materials Data, Inc.) X-ray pattern data processing software was used to determine the crystalline properties, including crystal size, and the full width at half-maximum (fwhm). Transmission electron microscopy and selected area electron diffraction data were attained on an FEI Tecnai 12 transmission electron microscope (TEM) operated at 120 kV. An FEI Quanta 200 environmental scanning electron microscope (ESEM) was used to acquire images of the wires and measure widths. All optical images were taken using a Nikon DS camera unit DS-L2 attached to an industrial Nikon ECLIPSE LV150 optical microscope.

AUTHOR INFORMATION

Corresponding Author:

*To whom correspondence should be addressed. E-mail: emenke@ucmerced.edu.

ACKNOWLEDGMENT This work was supported in part by the University of California Graduate and Research Council. Both J.E.H. and E.J.M. gratefully acknowledge Somnath Ghosh and Alan Sargisian at UC Merced for helpful discussions and advice.

REFERENCES

(1) Diezhandino, J.; Vergara, G.; Perez, G.; Genova, I.; Rodrigo, M. T.; Sanchez, F. J.; Torquemada, M. C.; Villamayor, V.; Plaza, J.; Catalan, I.; et al. Monolithic Integration of Spectrally Selective Uncooled Lead Selenide Detectors for Low Cost Applications. *Appl. Phys. Lett.* **2003,** *83*, 2751–2753.

(2) Kim, W. S.; Lee, J. H.; Park, Y. M.; Yoo, J. S.; Park, K. S. Development of Fast-Response Portable NDIR Analyzer Using Semiconductor Devices. *KSME Int. J.* **2003,** *17*, 2099–2106.

(3) Martin, J. M.; Hernandez, J. L.; Adell, L.; Rodriguez, A.; Lopez, F. Arrays of Thermally Evaporated PbSe Infrared Photodetectors Deposited on Si Substrates Operating at Room Temperature. *Semicond. Sci. Technol.* **1996,** *11*, 1740–1744.

(4) Rodrigo, M. T.; Sanchez, F. J.; Torquemada, M. C.; Villamayor, V.; Vergara, G.; Verdu, M.; Gomez, L. J.; Diezhandino, J.; Almazan, R.; Rodriguez, P.; et al. Polycrystalline Lead Selenide x−y Addressed Uncooled Focal Plane Arrays. *Infrared Phys. Technol.* **2003,** *44*, 281–287.

(5) Vergara, G.; Montojo, M. T.; Torquemada, M. C.; Rodrigo, M. T.; Sanchez, F. J.; Gomez, L. J.; Almazan, R. M.; Verdu, M.; Rodriguez, P.; Villamayor, V.; et al. Polycrystalline Lead Selenide: The Resurgence of an Old Infrared Detector. *Opto-Electron. Rev.* **2007,** *15*, 110–117.

(6) Zhou, F. L.; Li, X. M.; Gao, X. D.; Qiu, J. J. Low-Cost Preparation and Photoelectric Property Study of PbSe Nanocrystalline Films. *J. Inorg. Mater.* **2009,** *24*, 778–782.

(7) Chavez, J. A.; Ortega, J. A.; Perez, M. A.; Garcia, M. J. Low-Cost and Minimal-Conditioning Interface for a PbSe Photoconductor Array. *IEEE Trans. Instrum. Meas.* **1997,** *46*, 817–821.

(8) Masek, J.; Fach, A.; John, J.; Muller, P.; Paglino, C.; Zogg, H.; Buttler, W. Thermal Imaging Camera with Linear $Pb_{1-x}Sn_xSe$-on-Si Infrared Sensor Array and Combined JFET/CMOS Readout Electronics. *Nucl. Instrum. Methods Phys. Res., Sect. A* **1996,** *377*, 496–500.

(9) Zogg, H.; Alchalabi, K.; Zimin, D. Lead Chalcogenide, On Silicon Infrared Focal Plane Arrays for Thermal Imaging. *Def. Sci. J.* **2001,** *51*, 53–65.

(10) Zogg, H.; Fach, A.; John, J.; Masek, J.; Muller, P.; Paglino, C.; Buttler, W. $Pb_{1-x}Sn_xSe$-on-Si LWIR Sensor Arrays and Thermal Imaging with JFET/CMOS Read-out. *J. Electron. Mater.* **1996,** *25*, 1366–1370.

(11) Kimble, H. J. Near-Field Emission of Lead-Sulfide−Selenide Homojunction Lasers. *IEEE J. Quantum Electron.* **1980,** *16*, 740–743.

(12) Lo, W.; Swets, D. E. Diffused Homojunction Lead-Sulfide−Selenide Diodes with 140 K-Laser Operation. *Appl. Phys. Lett.* **1978,** *33*, 938–940.

(13) Pietryga, J. M.; Werder, D. J.; Williams, D. J.; Casson, J. L.; Schaller, R. D.; Klimov, V. I.; Hollingsworth, J. A. Utilizing the Lability of Lead Selenide to Produce Heterostructured Nanocrystals with Bright, Stable Infrared Emission. *J. Am. Chem. Soc.* **2008,** *130*, 4879–4885.

(14) Besson, J. M.; Paul, W.; Calawa, A. R. Tuning of Pbse Lasers by Hydrostatic Pressure from 8 to 22 Mu. *Phys. Rev.* **1968,** *173*, 699–713.

(15) Elizondo, L. A.; Li, Y.; Sow, A.; Kamana, R.; Wu, H. Z.; Mukherjee, S.; Zhao, F.; Shi, Z.; McCann, P. J. Optically Pumped Mid-Infrared Light Emitter on Silicon. *J. Appl. Phys.* **2007,** *101*, 104504–104506.

(16) Furst, J.; Pascher, H.; Schwarzl, T.; Boberl, M.; Springholz, G.; Bauer, G.; Heiss, W. Continuous-Wave Emission from Midinfrared IV−VI Vertical-Cavity Surface-Emitting Lasers. *Appl. Phys. Lett.* **2004,** *84*, 3268–3270.

(17) Malyarevich, A. M.; Savitsky, V. G.; Denisov, I. A.; Prokoshin, P. V.; Yumashev, K. V.; Raaben, E.; Zhilin, A. A.; Lipovskii, A. A. PbS(Se) Quantum Dot Doped Glass Applications As Laser Passive Q-Switches. *Phys. Status Solidi B* **2001,** *224*, 253–256.

(18) Springholz, G.; Schwarzl, T.; Heiss, W.; Bauer, G.; Aigle, M.; Pascher, H.; Vavra, I. Midinfrared Surface-Emitting PbSe/PbEuTe Quantum-Dot Lasers. *Appl. Phys. Lett.* **2001,** *79*, 1225–1227.

(19) Allan, G.; Delerue, C. Role of Impact Ionization in Multiple Exciton Generation in PbSe Nanocrystals. *Phys. Rev. B* **2006,** *73*, 205423–205428.

(20) Ellingson, R. J.; Beard, M. C.; Johnson, J. C.; Yu, P. R.; Micic, O. I.; Nozik, A. J.; Shabaev, A.; Efros, A. L. Highly Efficient Multiple Exciton Generation in Colloidal PbSe and PbS Quantum Dots. *Nano Lett.* **2005,** *5*, 865–871.

(21) Ji, M. B.; Park, S.; Connor, S. T.; Mokari, T.; Cui, Y.; Gaffney, K. J. Efficient Multiple Exciton Generation Observed in Colloidal PbSe Quantum Dots with Temporally and Spectrally Resolved Intraband Excitation. *Nano Lett.* **2009,** *9*, 1217–1222.

(22) Kim, S. J.; Kim, W. J.; Sahoo, Y.; Cartwright, A. N.; Prasad, P. N. Multiple Exciton Generation and Electrical Extraction from a PbSe Quantum Dot Photoconductor. *Appl. Phys. Lett.* **2008,** *92*, 031107–031110.

(23) Nair, G.; Geyer, S. M.; Chang, L. Y.; Bawendi, M. G. Carrier Multiplication Yields in PbS and PbSe Nanocrystals Measured by Transient Photoluminescence. *Phys. Rev. B* **2008,** *78*, 125325–125335.
(24) Nozik, A. J. Exciton Multiplication and Relaxation Dynamics in Quantum Dots: Applications to Ultrahigh-Efficiency Solar Photon Conversion. *Inorg. Chem.* **2005,** *44*, 6893–6899.
(25) Schaller, R. D.; Agranovich, V. M.; Klimov, V. I. High-Efficiency Carrier Multiplication through Direct Photogeneration of Multi-Excitons via Virtual Single-Exciton States. *Nat. Phys.* **2005,** *1*, 189–194.
(26) Noone, K. M.; Anderson, N. C.; Horwitz, N. E.; Munro, A. M.; Kulkarni, A. P.; Ginger, D. S. Absence of Photoinduced Charge Transfer in Blends of PbSe Quantum Dots and Conjugated Polymers. *ACS Nano* **2009,** *3*, 1345–1352.
(27) Ben-Lulu, M.; Mocatta, D.; Bonn, M.; Banin, U.; Ruhman, S. On the Absence of Detectable Carrier Multiplication in a Transient Absorption Study of InAs/CdSe/ZnSe Core/Shell1/Shell2 Quantum Dots. *Nano Lett.* **2008,** *8*, 1207–1211.
(28) Franceschetti, A. Structural and Electronic Properties of PbSe Nanocrystals from First Principles. *Phys. Rev. B* **2008,** *78*, 075418–075424.
(29) Luo, J. W.; Franceschetti, A.; Zunger, A. Carrier Multiplication in Semiconductor Nanocrystals: Theoretical Screening of Candidate Materials Based on Band-Structure Effects. *Nano Lett.* **2008,** *8*, 3174–3181.
(30) Pijpers, J. J. H.; Ulbricht, R.; Tielrooij, K. J.; Osherov, A.; Golan, Y.; Delerue, C.; Allan, G.; Bonn, M. Assessment of Carrier-Multiplication Efficiency in Bulk PbSe and PbS. *Nat. Phys.* **2009,** *5*, 811–814.
(31) Trinh, M. T.; Houtepen, A. J.; Schins, J. M.; Hanrath, T.; Piris, J.; Knulst, W.; Goossens, A. P. L. M.; Siebbeles, L. D. A. In Spite of Recent Doubts Carrier Multiplication Does Occur in PbSe Nanocrystals. *Nano Lett.* **2008,** *8*, 1713–1718.
(32) Kuno, M. An Overview of Solution-Based Semiconductor Nanowires: Synthesis and Optical Studies. *Phys. Chem. Chem. Phys.* **2008,** *10*, 620–639.
(33) Yashina, L. V.; Shtanov, V. I.; Yanenko, Z. G. The Application of VLS Growth Technique to Bulk Semiconductors. *J. Cryst. Growth* **2003,** *252*, 68–78.
(34) Zhu, J.; Peng, H. L.; Chan, C. K.; Jarausch, K.; Zhang, X. F.; Cui, Y. Hyperbranched lead Selenide Nanowire Networks. *Nano Lett.* **2007,** *7*, 1095–1099.
(35) Peng, X. S.; Meng, G. W.; Zhang, J.; Wang, X. F.; Wang, C. Z.; Liu, X.; Zhang, L. D. Strong Quantum Confinement in Ordered PbSe Nanowire Arrays. *J. Mater. Chem.* **2002,** *17*, 1283–1286.
(36) Sima, M.; Enculescu, I.; Sima, M.; Vasile, E. Semiconductor Nanowires Obtained by Template Method. *J. Optoelectron. Adv. Mater.* **2007,** *9*, 1551–1554.
(37) Wang, S. M.; Wang, C.; Zhang, M. Z.; Zong, Z. C.; Tian, H. F.; Liu, C.; Cao, J.; Zou, G. T. Electrode Position and Characterization of Quasi-One-Dimensional Lead/Lead Selenide Heterostructure Ordered Arrays. *J. Phys. Chem. C* **2009,** *113*, 16337–16341.
(38) Wang, W. H.; Geng, Y.; Qian, Y.; Ji, M. R.; Liu, X. M. A Novel Pathway to PbSe Nanowires at Room Temperature. *Adv. Mater.* **1998,** *10*, 1479–1481.
(39) Fardy, M.; Hochbaum, A. I.; Goldberger, J.; Zhang, M. M.; Yang, P. D. Synthesis and Thermoelectrical Characterization of Lead Chalcogenide Nanowires. *Adv. Mater.* **2007,** *19*, 3047–3051.
(40) Menke, E. J.; Thompson, M. A.; Xiang, C.; Yang, L. C.; Penner, R. M. Lithographically Patterned Nanowire Electrodeposition. *Nat. Mater.* **2006,** *5*, 914–919.
(41) Xiang, C. X.; Kung, S. C.; Taggart, D. K.; Yang, F.; Thompson, M. A.; Guell, A. G.; Yang, Y. A.; Penner, R. M. Lithographically Patterned Nanowire Electrodeposition: A Method for Patterning Electrically Continuous Metal Nanowires on Dielectrics. *Acs Nano* **2008,** *2*, 1939–1949.
(42) Yang, Y.; Kung, S. C.; Taggart, D. K.; Xiang, C.; Yang, F.; Brown, M. A.; Guell, A. G.; Kruse, T. J.; Hemminger, J. C.; Penner, R. M. Synthesis of PbTe Nanowire Arrays Using Lithographically Patterned Nanowire Electrodeposition. *Nano Lett.* **2008,** *8*, 2447–2451.
(43) Saloniemi, H.; Kanniainen, T.; Ritala, M.; Leskela, M.; Lappalainen, R. Electrodeposition of Lead Selenide Thin Films. *J. Mater. Chem.* **1998,** *8*, 651–654.
(44) Saloniemi, H.; Kemell, M.; Ritala, M.; Leskela, M. Electrochemical Quartz Crystal Microbalance and Cyclic Voltammetry Studies on PbSe Electrodeposition Mechanisms. *J. Mater. Chem.* **2000,** *10*, 519–525.
(45) Yang, F.; Taggart, D. K.; Penner, R. M. Fast, Sensitive Hydrogen Gas Detection Using Single Palladium Nanowires That Resist Fracture. *Nano Lett.* **2009,** *9*, 2177–2182.
(46) Sashchiuk, A.; Amirav, L.; Bashouti, M.; Krueger, M.; Sivan, U.; Lifshitz, E. PbSe Nanocrystal Assemblies: Synthesis and Structural, Optical, And Electrical Characterization. *Nano Lett.* **2004,** *4*, 159–165.

DOI: 10.1021/jz100173a | *J. Phys. Chem. Lett.* **2010,** *1*, 1055–1059